Am J Cancer Res 2026;16(7):2725-2739
www.ajcr.us /ISSN:2156-6976/ajcr0173959

Original Article

Risk factors for cardiac dysfunction caused by anthracycline drugs in the treatment of lymphoma and the early monitoring value of three-dimensional echocardiography

Jing Jiang*, Xiaolei Mu*, Xiaomei Chen, Qianqian Li

*Department of Cardiac Ultrasound, Qingdao Municipal Hospital, Qingdao 266000, Shandong, China. *Equal contributors.*

Received May 11, 2026; Accepted June 17, 2026; Epub July 15, 2026; Published July 30, 2026

Abstract: Anthracyclines (ANTs) are important chemotherapeutic drugs for the treatment of lymphoma. However, its cardiotoxicity poses a challenge to its continued use. The development of ARCD is influenced by multiple factors, making early detection challenging. Three-dimensional speckle tracking imaging (3D-STI) can quantitatively analyze myocardial strain by tracking the movement of myocardial spots. This study compared the parameters derived from conventional echocardiography, 3D-STI, and three-dimensional echocardiography at baseline (T0), 2 cycles of chemotherapy (T2) and 4 cycles of chemotherapy (T4), and analyzed the risk factors for ARCD. From January 2020 to December 2024, a total of 189 patients with non-Hodgkin lymphoma were recruited, all of whom received at least 4 cycles of ANT treatment. During chemotherapy and follow-up, 28 patients developed ARCD. Firth-penalized logistic regression demonstrated that age ≥65 years (aOR = 3.416, 95% CI: 1.241-9.913), hypertension (aOR = 3.051, 95% CI: 1.095-8.675), and cumulative ANT dose (aOR = 1.028, 95% CI: 1.017-1.040) were independently associated with an increased risk of ARCD. Conventional echocardiographic parameters, including LVEF, showed no significant changes. Compared with T0, right ventricular end-diastolic volume (RVEDV) and right ventricular end-systolic volume (RVESV) were significantly increased at T4 ($P<0.05$), left ventricular global longitudinal strain (LVGLS) was significantly decreased at T2 ($P<0.05$), and left ventricular global circumferential strain (LVGCS) was significantly decreased at T4 ($P<0.05$). The absolute change in LVGLS from T0 to T2 (ΔLVGLS) was significantly and positively correlated with the cumulative ANT dose ($R = 0.336$, $P<0.001$). The cut-off value for predicting ARCD using ΔLVGLS was 3.5%. The area under the curve (AUC) was 0.852 and the respective sensitivity and specificity were 0.929 and 0.739. 3D-STI, particularly LVGLS, demonstrated significant value in the early identification of cardiac dysfunction in patients with lymphoma undergoing ANT treatment.

Keywords: Lymphoma, non-Hodgkin lymphoma, anthracycline drugs, heart injury, risk factors, three dimensional speckle tracking

Introduction

Lymphoma is a common malignancy of the hematologic system. Its incidence has increased significantly in recent years. It ranks among the ten most common cancers worldwide [1]. Non-Hodgkin lymphoma (NHL) accounts for approximately 90% of all lymphoma cases, whereas Hodgkin lymphoma (HL) represents only a small proportion [2]. Anthracyclines (ANTs), including doxorubicin, daunorubicin, and epirubicin, are highly effective chemotherapeutic agents widely used in the treatment of lymphoma and other malignancies [3]. However, they are associated with dose-dependent cardiotoxicity and may lead to long-term complications such as heart failure or cardiomyopathy [4]. The risk of cardiotoxicity in adults using ANTs is 3% to 20%, and the incidence is higher in children, ranging from 2% to 65% [5]. Cardiotoxicity is usually defined as a decrease in left ventricular ejection fraction (LVEF) from baseline of ≥10% from baseline to a value below 50% [6]. The three types of cardiac toxic-

https://doi.org/10.62347/GOZT5673

ity induced by chemotherapeutic drugs are acute, chronic and delayed. Chronic cardiotoxicity mostly occurs within 1 year after treatment. In contrast, acute symptoms that occur during or shortly after treatment are rare, with an incidence of less than 1% [7]. Compared with other more common heart diseases, ANT-induced cardiomyopathy has a very poor prognosis, with a mortality rate of up to 60% within 2 years [8]. The mechanism of ANT-related cardiotoxicity is complex, involving oxidative stress, mitochondrial dysfunction, calcium dysregulation, cell death pathway disorders and DNA damage [5]. The use of liposomal ANTs can significantly reduce severe cardiotoxicity compared to conventional formulations [9]. However, even low-dose ANTs can still cause asymptomatic cardiac damage. Currently, there is no fully effective way to prevent or treat cardiotoxicity. Dexrazoxane is currently the only cardiac protective agent approved by the U.S. Food and Drug Administration for use in preventing cardiotoxicity caused by ANTs [10]. However, it has not been widely used in clinical practice due to its high cost and dosage, which can lead to bone marrow toxicity and complicate treatment during chemotherapy [11]. Therefore, it is of great clinical significance to evaluate and monitor patients for risk factors before or during ANTs use, especially with regard to the early detection of cardiac function injury.

Routine monitoring methods for ANT-related cardiotoxicity include myocardial injury markers, electrocardiograms, echocardiography and cardiac magnetic resonance imaging. Serum myocardial markers, such as B-type natriuretic peptide and troponin, may be insufficiently sensitive in the early stages of cardiac injury. LVEF, as measured by conventional two-dimensional echocardiography, only decreases significantly when there were organic lesions in the heart. When LVEF is less than 50%, heart damage is irreversible, which is insufficient for early warning purposes. In contrast, new technologies such as three-dimensional echocardiography and three-dimensional speckle tracking imaging (3D-STI) have significant advantages. Studies have shown that 3D-STI parameters can sensitively capture early myocardial damage caused by ANT-related cardiotoxicity in breast cancer [12]. However, there are few reports on the early detection of cardiac function damage caused by ANTs in lymphoma patients. This study examined lymphoma patients who had been treated with ANTs. The risk factors for cardiac function damage were analyzed retrospectively, and the clinical value of 3D-STI in the early identification of myocardial injury was discussed. The aim was to provide a scientific basis for optimizing treatment plans.

Materials and methods

Research subjects

This was a single-center, retrospective study. Patients with newly diagnosed NHL who were admitted to Qingdao Municipal Hospital from 1 January 2020 to 31 December 2024 were included in the study. The Medical Ethics Committee of Qingdao Municipal Hospital reviewed the study.

Inclusion criteria: Patients aged 18 years or older with a confirmed pathological diagnosis of NHL who had received at least four cycles of standard first-line CHOP or R-CHOP chemotherapy, and who had an Eastern Cooperative Oncology Group Performance Status (ECOG PS) score of 0-2. The estimated survival time was greater than six months. Patients signed informed consent forms and were able to cooperate with the completion of examinations and follow-ups during the study.

Exclusion criteria: LVEF ≤55% as determined by two-dimensional echocardiography prior to chemotherapy; patients with heart failure (NYHA II-IV) or other heart diseases requiring long-term hospitalization who had clear symptoms prior to chemotherapy; patients who underwent chest radiotherapy within 12 months prior to chemotherapy. Patients with factors affecting the quality of ultrasound images that make it impossible to accurately evaluate LVEF; pregnant or lactating women.

Chemotherapeutic regimens

The CHOP regimen consisted of 21-day cycles. On day 1, patients received an intravenous infusion containing cyclophosphamide (750 mg/m^2), doxorubicin (50 mg/m^2), and vincristine (1.4 mg/m^2, capped at 2.0 mg). Oral pred-

nisone (100 mg/m^2) was administered daily from day 1 through day 5. Depending on clinical response and individual treatment strategies, patients underwent 4 to 8 cycles in total.

Patients received the R-CHOP regimen on a 21-day cycle. Rituximab (375 mg/m^2) was infused intravenously on day 1, followed by intravenous cyclophosphamide (750 mg/m^2), doxorubicin (50 mg/m^2), and vincristine (1.4 mg/m^2, capped at 2.0 mg) on day 2. Oral prednisone (100 mg/m^2) was administered daily from day 1 through day 5. A total of 4 to 8 cycles were delivered per patient according to the individualized treatment plan.

Echocardiographic protocol and image analysis

Image acquisition protocol: Echocardiographic examinations were performed at three distinct time points: prior to chemotherapy initiation (T0), following two cycles (T2), and after four cycles (T4) of chemotherapy. All examinations were conducted using a GE Vivid E95 ultrasound system equipped with 4V and M5Sc transducers. Patients were examined in the left lateral decubitus position during quiet respiration. Standardized image acquisition was performed by two experienced sonographers following established protocols to ensure consistency. All acquired images and data were stored in DICOM format for subsequent offline analysis.

Conventional echocardiographic parameters: Initial imaging was performed with continuous electrocardiographic gating using a 2-5 MHz M5Sc transducer positioned at the apical four-chamber, apical two-chamber, and parasternal long-axis views. From each view, 3-5 consecutive cardiac cycles were acquired as two-dimensional grayscale cine loops (frame rate 55-90 frames/s) and M-mode recordings. Left ventricular end-diastolic dimension (LVEDD) and left ventricular end-systolic dimension (LVESD) were measured at end-diastole and end-systole, respectively. Left ventricular ejection fraction (LVEF) was then calculated using the biplane Simpson's method from the apical four- and two-chamber views.

Doppler hemodynamic assessment: Pulsed-wave Doppler was performed with the sample volume placed at the left ventricular side of the mitral valve orifice in the apical four-chamber view to measure the peak early (LV E) and late (LV A) diastolic filling velocities, from which the LV E/A ratio was calculated. Similarly, the sample volume was positioned at the right ventricular side of the tricuspid valve orifice to obtain the peak early (RV E) and late (RV A) diastolic filling velocities and calculate the RV E/A ratio. Right ventricular function was evaluated by manually tracing the endocardial borders of the right ventricle in the apical four-chamber view at end-diastole and end-systole to calculate the right ventricular fractional area change (RVFAC).

Three-dimensional volumetric analysis: A 4V transducer was used to acquire full-volume datasets from the apical four-chamber view during a single breath-hold, capturing three consecutive cardiac cycles with a volume frame rate >30% of the heart rate. The datasets were transferred to an EchoPAC workstation and analyzed offline using the 4D Auto LVQ application. The software automatically identified the left ventricular endocardial borders throughout the cardiac cycle, with manual correction performed when necessary, to compute the left ventricular end-diastolic volume (LVEDV), left ventricular end-systolic volume (LVESV), and right ventricular volumes, including end-diastolic (RVEDV) and end-systolic (RVESV) values.

Speckle-tracking strain analysis: 3D-STI was performed using high-frame-rate, full-volume images obtained from the apical four-chamber view, with three consecutive cardiac cycles recorded for each view. Offline analysis was conducted using EchoPAC software. After manual initialization of the left ventricular endocardial border at end-systole, the software automatically tracked myocardial motion in three dimensions throughout the cardiac cycle to compute global longitudinal strain (LVGLS) and global circumferential strain (LVGCS), as shown in **Figure 1**. The absolute difference in LVGLS between the T0 and T2 time points was defined as ΔLVGLS.

Consistency assessment: The Bland-Altman method was used to evaluate the consistency of 3D-STI layered strain examination. The study

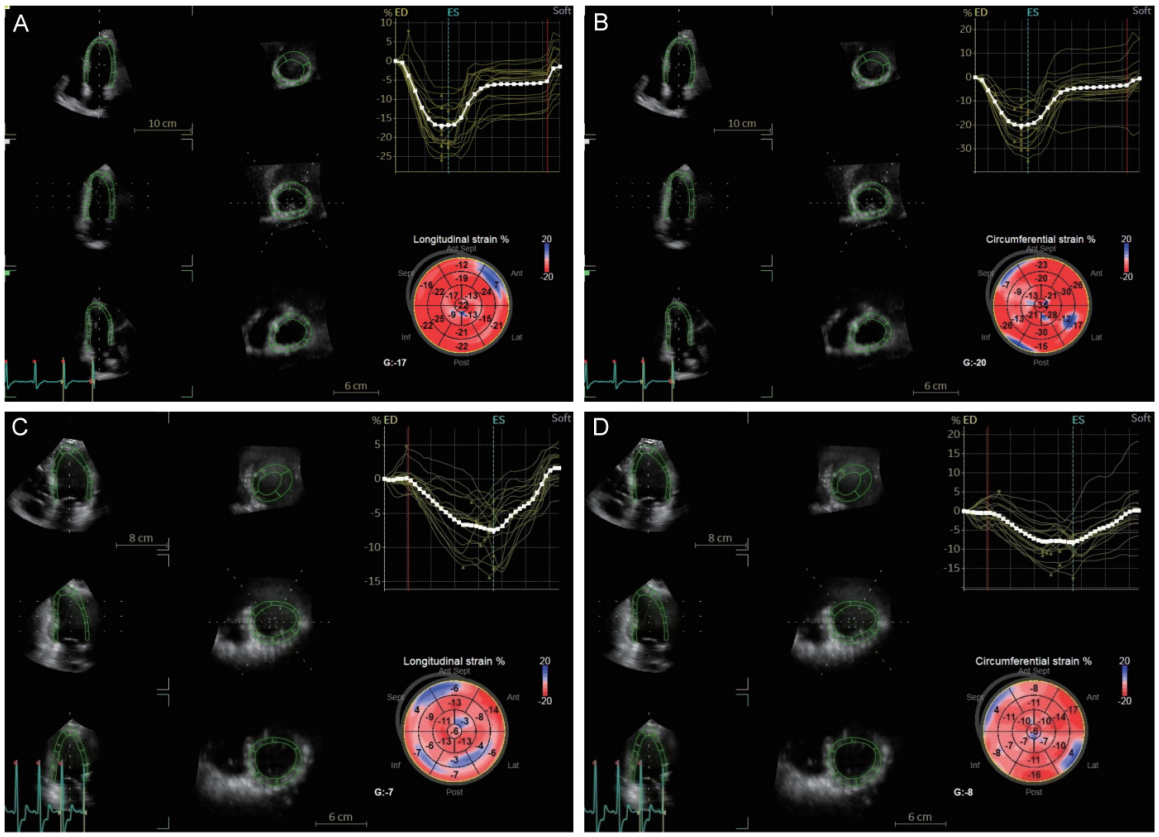

Figure 1. 3D-STI images showing LVGLS (A, C) and LVGCS (B, D) in an NHL patient. (A, B) Baseline (T0) before chemotherapy; (C, D) After 4 cycles of chemotherapy (T4).

included 20 patients, and two experienced physicians independently completed image acquisition and data analysis. The evaluation types included the intra-observer consistency of the same physician's two measurements and the inter-observer consistency of the two physicians' measurements. Using LVGLS and LVGCS as indicators, the limits of agreement were defined as the mean difference ± 1.96 standard deviations of the differences between the two measurements. If the proportion of measurements that exceed this limit is less than 10%, the consistency of the indicator is judged to be good [13].

Information collection and biochemical parameters: Baseline patient characteristics were collected prior to treatment, including age, gender, body mass index (BMI), smoking, drinking, and cardiovascular risk factors (including hypertension, diabetes, and dyslipidemia). Disease-related data included pathological type, Ann Arbor stage, cumulative dose of ANT, Ki-67, and International Prognostic Index (IPI) [14]. Baseline (T0) biochemical parameters were collected prior to chemotherapy, including hemoglobin (Hb), albumin (Alb), serum creatinine (Scr), serum uric acid (SUA), alanine aminotransferase (ALT) and aspartate aminotransferase (AST).

Outcome

The primary endpoint of the study was ANT related cardiac dysfunction (ARCD) during chemotherapy and within 12 months after chemotherapy [15]. ARCD was defined based on two-dimensional echocardiography as either an absolute decrease in LVEF of ≥5% from baseline with a follow-up LVEF <55%, or an absolute decrease in LVEF of ≥10% from baseline with a follow-up LVEF <50%.

Statistical method

SPSS 27.0 was used for all statistical analyses. Normally distributed quantitative variables are shown as mean ± standard deviation (SD)

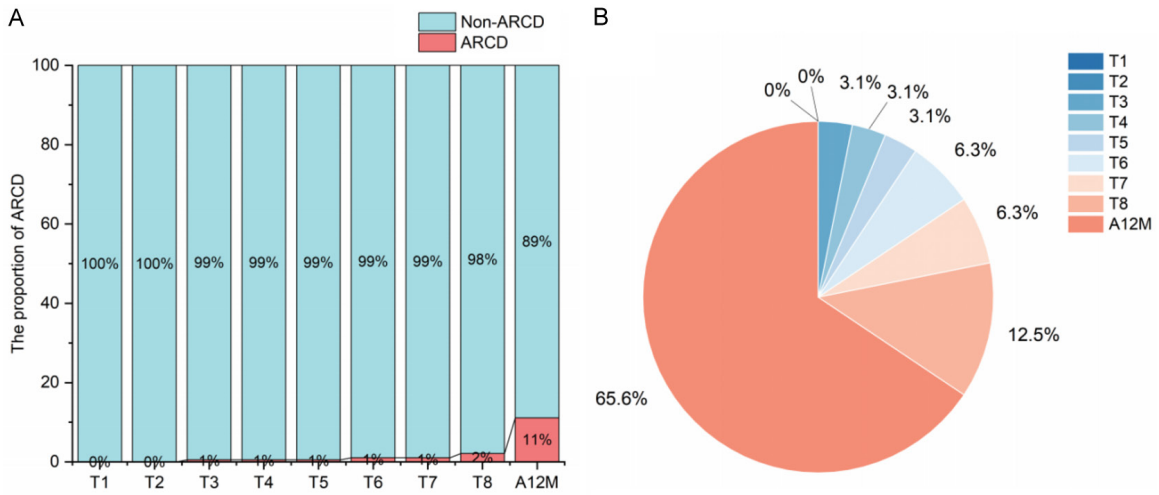

Figure 2. The time distribution characteristics of anthracycline-related cardiac dysfunction (T1-T8 chemotherapy cycle and A12M follow-up). A. The number distribution of patients with ARCD at each time point; B. The proportion distribution of 28 patients with ARCD at each time point. Abbreviation: ARCD, anthracycline-related cardiac dysfunction; A12M, 12-month follow-up after treatment.

and compared using the t-test. Qualitative variables are expressed as n (%) and analyzed with the χ^2 test. Repeated measures analysis of variance (ANOVA) was used to compare echocardiographic parameters across the three time points (T0, T2, and T4). Logistic regression was used to analyze the influencing factors of cardiac dysfunction in NHL patients. Spearman's rank correlation coefficient was used to evaluate the correlation between the variables. The relationship between the dose of ANTs received by patients and the risk of developing ARCD was investigated using restricted cubic spline (RCS) analysis. Longitudinal changes in LVGLS were analyzed using generalized estimating equations (GEE). The predictive value of variables for ARCD was evaluated using receiver operating characteristic curve (ROC) analysis. Multivariable logistic regression was performed using Firth-penalized logistic regression (logistf package in R) due to the limited number of ARCD events. To minimize overfitting, only variables with a statistically significant association in univariable analysis were included in the final model. A *p*-value <0.05 was considered statistically significant.

Results

Clinical characteristics

Eight patients were under 18 years of age. Three patients were excluded due to abnormal myocardial markers prior to chemotherapy. Sixteen patients were excluded due to receiving fewer than four courses of chemotherapy. Twenty-six patients were excluded due to a lack of complete blood test results or echocardiography parameters. This study finally included a total of 189 patients, with 86 male and 103 female, aged between 24 and 87 years, with an average age of 56.07±13.84 years. Of these patients, 142 had diffuse large B-cell lymphoma, 21 had follicular lymphoma, nine had mantle cell lymphoma, and 17 had peripheral T-cell lymphoma. All patients included had newly diagnosed NHL and completed at least four cycles of CHOP or R-CHOP chemotherapy. Among them, 21 patients (11.1%), 32 patients (16.9%), 84 patients (44.4%), 27 patients (14.3%) and 25 patients (13.2%) completed 4, 5, 6, 7 and 8 courses of treatment, respectively. During the follow-up period, a total of 32 ARCD events were recorded, with four patients experiencing two events each. A total of 28 patients (14.81%) developed ARCD. Among them, 65.6% developed ARCD during the 12-month follow-up after chemotherapy completion, presenting predominantly as subacute or early-onset cardiotoxicity (**Figure 2**). During the study, no patients received cardiotoxic therapy, radiation therapy, or cardioprotective medication, and no one developed signs or symptoms of heart failure.

Table 1. Comparison of clinical characteristics between the two groups

Variables	Total (n = 189)	ARCD (n = 28)	Non-ARCD (n = 161)	t/χ^2	*P*
Age, yr, n (%)				16.070	<0.001
<65	118 (62.43)	8 (28.57)	110 (68.32)		
≥65	71 (37.57)	20 (71.43)	51 (31.68)		
Gender, n (%)				0.512	0.474
Male	86 (45.50)	11 (39.29)	75 (46.58)		
Female	103 (54.50)	17 (60.71)	86 (53.42)		
BMI, kg/m^2, n (%)				0.018	0.894
<24	133 (70.37)	20 (71.43)	113 (70.19)		
≥24	56 (29.63)	8 (28.57)	48 (29.81)		
Smoking history, n (%)				0.739	0.390
Yes	61 (32.28)	11 (39.29)	50 (31.06)		
No	128 (67.72)	17 (60.71)	111 (68.94)		
Drinking history, n (%)				1.650	0.119
Yes	43 (22.75)	9 (32.14)	34 (21.12)		
No	146 (77.25)	19 (67.86)	127 (78.88)		
Hypertension, n (%)				11.191	<0.001
Yes	52 (27.51)	15 (53.57)	37 (22.98)		
No	137 (72.49)	13 (46.43)	124 (77.02)		
Diabetes, n (%)				3.969	0.046
Yes	30 (15.87)	8 (28.57)	22 (13.66)		
No	159 (84.13)	20 (71.43)	139 (86.34)		
Dyslipidemia, n (%)				1.264	0.261
Yes	39 (20.63)	8 (28.57)	31 (19.25)		
No	150 (79.37)	20 (71.43)	130 (80.75)		
Tumor type, n (%)				1.587	0.662
DLBCL	142 (75.13)	21 (75.00)	121 (75.16)		
FL	21 (11.11)	2 (7.14)	19 (11.80)		
MCL	9 (4.76)	1 (3.57)	8 (4.97)		
PTCL	17 (9.00)	4 (14.29)	13 (8.07)		
Ann Arbor stage, n (%)				1.015	0.314
I-II	84 (44.44)	10 (35.71)	74 (45.96)		
III-IV	105 (55.56)	18 (64.29)	87 (54.04)		
IPI, n (%)				5.113	0.024
0-2	146 (77.25)	17 (60.71)	129 (80.12)		
3-5	43 (22.75)	11 (39.29)	32 (19.88)		
Ki-67, %, n (%)				3.224	0.073
<65	69 (36.51)	6 (21.43)	63 (39.13)		
≥65	120 (63.49)	22 (78.57)	98 (60.87)		
Accumulated dose of ANTs, mg/m^2, Mean ± SD	295.90±62.31	367.86±45.57	283.39±56.11	7.540	<0.001
HB, g/L, Mean ± SD	124.25±18.29	122.93±13.38	124.48±18.64	0.415	0.679
Alb, g/L, Mean ± SD	41.04±5.75	41.91±7.03	40.89±5.51	0.870	0.386
Scr, umol/L, Mean ± SD	58.11±14.37	61.76±14.33	57.47±14.32	1.462	0.146
SUA, μmol/L, Mean ± SD	324.79±85.01	327.79±88.49	324.27±84.67	0.202	0.840
ALT, U/L, Mean ± SD	17.28±7.78	19.93±6.93	16.93±7.89	1.468	0.144
AST, U/L, Mean ± SD	19.69±6.68	20.43±6.91	19.56±6.65	0.634	0.527

Note: Values are mean ± SD, n, or n (%). The p values compare ARCD with Non-ARCD. Abbreviation: ARCD, anthracycline-related cardiac dysfunction; BMI, body mass index; DLBCL, diffuse large B-cell lymphoma; FL, follicular lymphoma; MCL, mantle cell lymphoma; PTCL, peripheral T-cell lymphoma; IPI, international prognostic index; ANTs, anthracyclines; Hb, hemoglobin; Alb, albumin; Scr, serum creatinine; SUA, serum uric acid; ALT, alanine aminotransferase; AST, aspartate aminotransferase.

Table 2. Results of Firth-penalized multivariable logistic regression

Variables	*β*	SE	*aOR* (95% *CI*)	*P* value
Age ≥65 y	1.229	0.517	3.416 (1.241-9.913)	0.017
Hypertension	1.115	0.515	3.051 (1.095-8.675)	0.033
Accumulated dose of ANTs	0.027	0.005	1.028 (1.017-1.040)	<0.001

Note: Age <65 yr = 0, hypertension no = 0. Abbreviation: aOR, adjusted odds ratio; ANTs, anthracyclines.

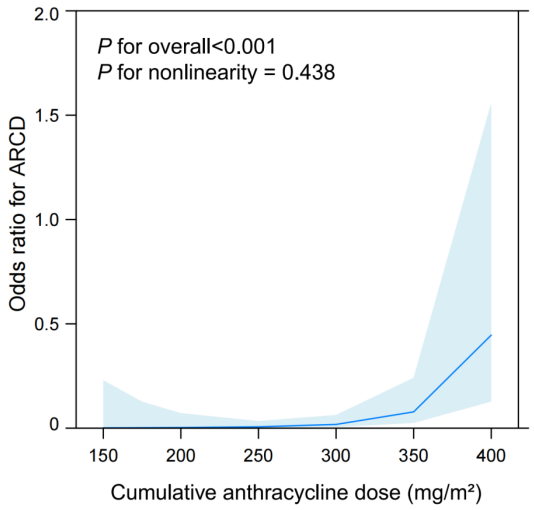

Figure 3. A linear correlation between cumulative anthracycline dose and ARCD risk.

Factors analysis

Table 1 shows the patient demographics and clinical characteristics. The mean cumulative ANT dose was 295.90±62.31 mg/m^2. The proportion of patients who were aged ≥65 years, had hypertension or diabetes, or had an IPI score of 3-5 was higher in the ARCD group than in the non-ARCD group. Given the limited number of ARCD events (n = 28), multivariable analysis was restricted to variables with a statistically significant association in univariable analysis: age, hypertension, and cumulative ANT dose. Collinearity was assessed and no multicollinearity was observed (VIF <10). Firth-penalized logistic regression demonstrated that age ≥65 years (aOR = 3.416, 95% CI: 1.241-9.913), hypertension (aOR = 3.051, 95% CI: 1.095-8.675), and cumulative ANT dose (aOR = 1.028, 95% CI: 1.017-1.040) were independently associated with an increased risk of ARCD (**Table 2**).

Cumulative ANT dose is linearly associated with ARCD risk

RCS analysis demonstrated a significant dose-response relationship between cumulative ANT dose and ARCD risk (*P*<0.001), with no evidence of nonlinearity (*P* for nonlinearity = 0.438), as shown in **Figure 3**. ARCD incidence increased with dose: 0% at <240 mg/m^2, 5.4% at 240-299 mg/m^2, 19.2% at 300-399 mg/m^2, and 68.0% at ≥400 mg/m^2.

Interaction analysis of risk factors for ARCD

No significant interaction was observed between age and cumulative ANT dose (*P* for interaction = 0.322), or between hypertension and cumulative ANT dose (*P* = 0.313). A borderline interaction between age and hypertension was observed (*P* = 0.089), suggesting a potential combined effect, although it did not reach statistical significance, as shown in **Figure 4**.

Comparison of ultrasonic parameters before and after chemotherapy

There was no significant difference in LVEDD, LVESD, LV E, LV A, RV E/A ratio, RV E, RV A, RV E/A ratio, RVFAC, LVEF, LVEDV, LVESV between before and after chemotherapy (*P*>0.05). Compared with T0, RVEDV and RVESV were significantly increased at T4 (*P*<0.05). Compared with T0, LVGLS decreased significantly at T2, and LVGCS decreased significantly at T4 (*P*< 0.05), as shown in **Table 3**.

GEE analysis of LVGLS changes

GEE analysis revealed significant time-by-group interactions for LVGLS at both T2 (β = 4.182, P<0.001) and T4 (β = 2.391, P<0.001), indicating that the change in LVGLS over time differed significantly between the ARCD and non-

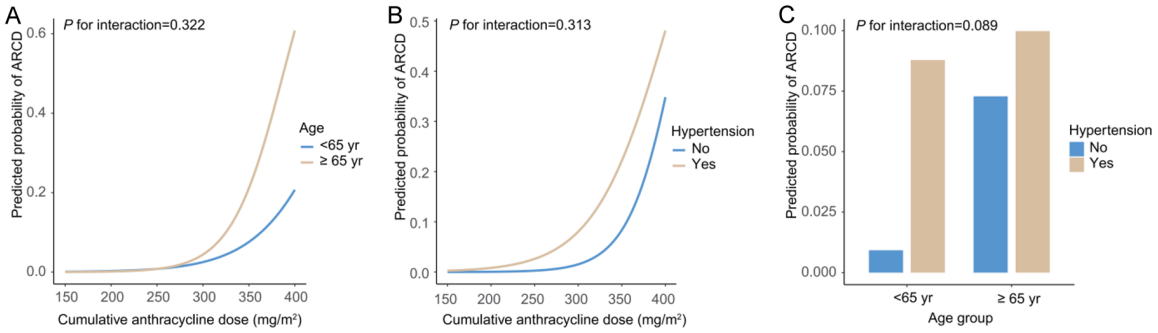

Figure 4. Interaction analysis. A. Interaction between age and cumulative anthracycline dose; B. Interaction between hypertension and cumulative anthracycline dose; C. Interaction between age and hypertension.

Table 3. Comparison of ultrasound parameters before and after chemotherapy

Parameters	T0	T2	T4	*F*	*P*
LVEDD (mm)	45.76±2.44	45.35±2.77	45.28±2.63	1.856	0.157
LVESD (mm)	28.31±2.64	28.43±2.10	28.75±1.96	1.916	0.148
LV E (cm/s)	64.88±11.59	64.22±11.89	62.82±10.80	1.602	0.202
LV A (cm/s)	64.65±12.53	65.42±11.59	65.91±14.26	0.462	0.630
LV E/A ratio	1.04±0.26	1.01±0.27	0.99±0.24	1.799	0.166
RV E (cm/s)	55.29±7.61	54.95±8.90	54.66±8.11	0.278	0.757
RV A (cm/s)	51.91±10.80	52.63±11.71	52.85±12.40	0.336	0.715
RV E/A ratio	1.12±0.30	1.10±0.33	1.12±0.50	0.152	0.859
RVFAC (%)	41.82±5.50	41.38±5.11	41.50±5.37	0.495	0.610
LVEF (%)	62.61±4.38	61.81±4.11	61.94±4.03	2.009	0.135
LVEDV (mL)	77.56±10.19	78.45±10.61	78.96±9.80	0.914	0.401
LVESV (mL)	30.59±7.50	31.18±6.80	30.99±6.60	0.349	0.706
RVEDV (mL)	58.66±7.80	59.43±7.29	60.68±7.00*	3.618	0.027
RVESV (mL)	27.72±4.50	28.47±3.97	29.40±4.40*	7.194	<0.001
LVGLS (%)	-20.78±3.85	-19.88±3.04*	-18.25±2.75*,#	29.564	<0.001
LVGCS (%)	-19.41±3.03	-18.95±3.07	-17.92±3.03*,#	12.014	<0.001

Note: Values are mean ± SD, *Compared with T0, P<0.05, #Compared with T2, P<0.05. Abbreviation: LVEDD, left ventricular end-diastolic dimension; LVESD, left ventricular end-systolic dimension; LV, left ventricle; RV, right ventricle; E, peak inflow velocity of early diastolic filling; A, peak inflow velocity of late diastolic filling; RVFAC, right ventricular fractional area change; LVEF, left ventricular ejection fraction; LVEDV, left ventricular end-diastolic volume; LVESV, left ventricular end-systolic volume; RVEDV, right ventricular end-diastolic volume; RVESV, right ventricular end-systolic volume; LVGLS, left ventricular global longitudinal strain; LVGCS, left ventricular global circumferential strain; T0 = baseline before chemotherapy; T2 = after 2 cycles of chemotherapy; T4 = after 4 cycles of chemotherapy.

ARCD groups, as shown in **Table 4**. The ARCD group exhibited a sharp decline in LVGLS from T0 to T2 (absolute value decreased by 4.54%), whereas the non-ARCD group showed minimal change (absolute value decreased by 0.35%), as shown in **Figure 5**.

Subgroup analysis of ΔLVGLS and its correlation with cumulative ANT dose

In the overall cohort, LVGLS at T2 was significantly lower than that at T0 in both age subgroups (<65 years and ≥65 years) and both genders, indicating that early ANT-induced subclinical myocardial injury is a universal phenomenon. However, when comparing the magnitude of change (ΔLVGLS) between subgroups, no significant difference was observed between different ages or genders. In contrast, patients with a cumulative ANT dose ≥240 mg/m^2 showed not only a significant decrease in LVGLS at T2 but also a greater ΔLVGLS compared with those receiving <240 mg/m^2 (P< 0.05), as shown in **Figure 6**.

Table 4. GEE analysis of LVGLS longitudinal changes between ARCD and non-ARCD groups

	β	SE	Wald χ^2	*P* value
Intercept	-20.186	0.283	5077.12	<0.001
Time (T2 vs. T0)	0.354	0.225	2.480	0.115
Time (T4 vs. T0)	2.180	0.214	103.72	<0.001
Group (ARCD vs. Non-ARCD)	-4.028	0.701	32.98	<0.001
Time T2 × Group ARCD	4.182	0.296	199.81	<0.001
Time T4 × Group ARCD	2.391	0.621	14.810	<0.001

Note: Abbreviation: GEE, generalized estimating equations; CI, confidence interval; LVGLS, left ventricular global longitudinal strain; ARCD, anthracycline-related cardiac dysfunction.

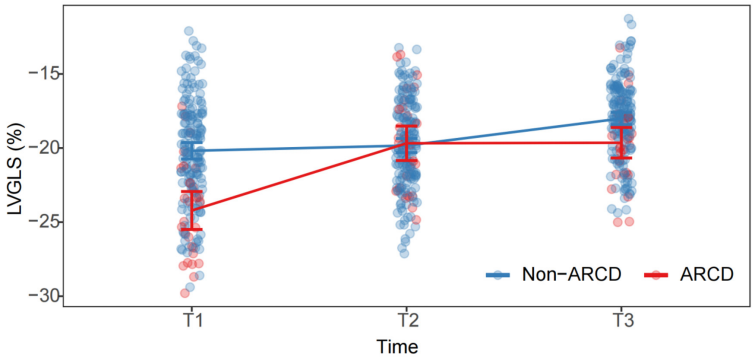

Figure 5. Longitudinal trajectories of LVGLS in patients with and without ARCD.

Spearman correlation analysis was used to analyze the correlation between ΔLVGLS and accumulated dose of ANTs in patients. **Figure 7** shows a significant positive relationship between ΔLVGLS and the total dose of ANTs (R = 0.336, P<0.001), as revealed by correlation analysis.

The predictive value of ΔLVGLS for ARCD

The cut-off value for predicting ARCD using ΔLVGLS was 3.5%. The AUC was 0.852, with respective sensitivity and specificitys of 0.929 and 0.739. The AUC of ΔLVGLS combined with age, hypertension and cumulative dose of ANT to predict ARCD was 0.947, and the sensitivity and specificity were 0.857 and 0.913, respectively, as shown in **Figure 8**.

Conformance testing

As shown in **Figure 9**, LVGLS and LVGCS exhibited good consistency within and between observers. With "mean ± 1.96 standard deviation" as the consistency limit, less than 10% of LVGLS and LVGCS parameters exceeded this interval. Among these parameters, LVGLS had only one abnormal value in the intra-operator evaluation. In the inter-operator evaluation, neither LVGLS nor LVGCS had any abnormal values.

Discussions

ANTs are a well-known type of antitumour drug, but they can also have a negative impact on the heart. ANTs-induced myocardial toxicity is a chronic cumulative process, usually within 1 year after the end of chemotherapy, it gradually appears as a significant decline in cardiac function [7]. Our data confirm that ARCD follows a staged progression. The 12-month post-treatment follow-up period was when ARCD occurred most frequently, a finding consistent with previous reports [16]. In addition, our study found that cumulative ANT dose, hypertension, and age were risk factors for ARCD. The relationship between the cumulative dose of ANTs and cardiac dysfunction has been fully established [17]. Previous studies have shown that higher cumulative doses are associated with increased risk of ANTs-related cardiotoxicity [18]. Doxorubicin is the most commonly used ANT. The cumulative dose of doxorubicin ≥240 mg/m^2 has been classified as a risk factor for cardiac dysfunction. Studies have shown that cumulative doxorubicin doses of 400, 550, and 700 mg/m^2 correspond to cardiotoxicity risks of approximately 5%, 26%, and nearly 50%, respectively [19]. In this study, the maximum cumulative dose of doxorubicin was 400 mg/m^2, which was lower than the upper limit recommended by the guidelines (400-450 mg/m^2) [20]. However, 14.8% of patients still developed ARCD, indicating that cardiac toxicity cannot be ignored even within a relatively safe dose range. Hypertension, in addition to being a major risk factor for heart failure, significantly

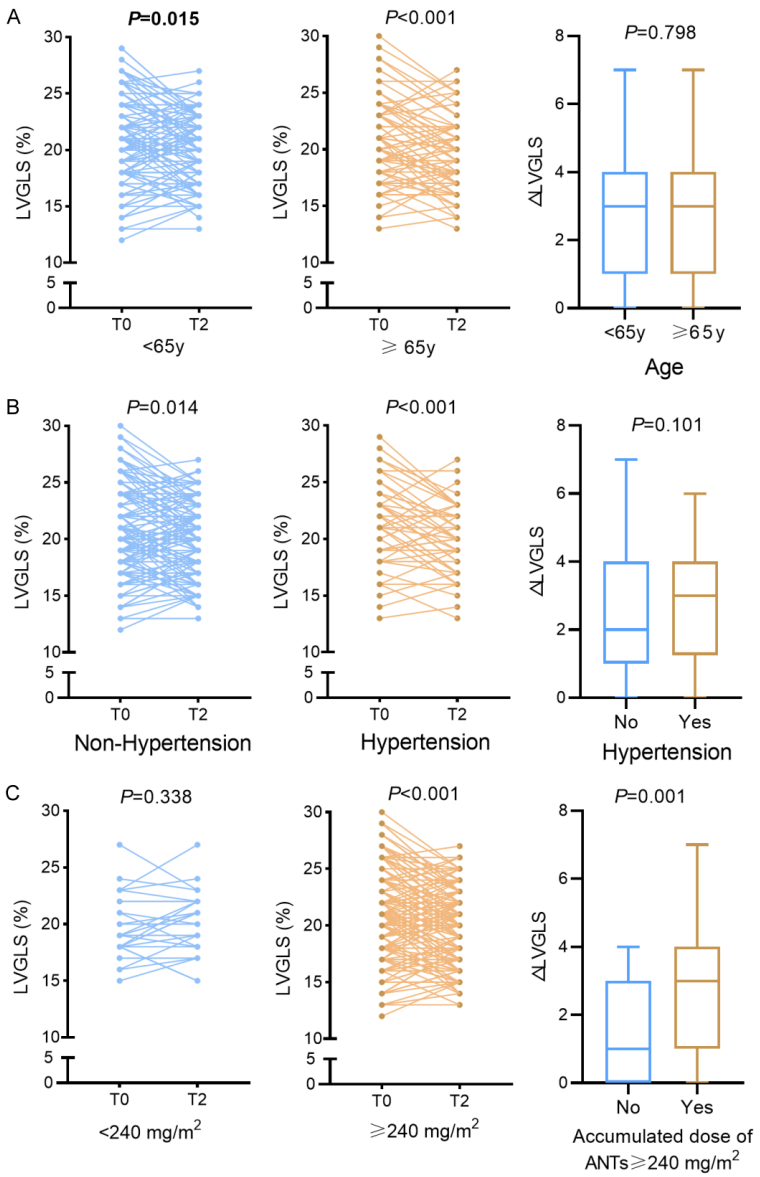

Figure 6. Subgroup analysis of ΔLVGLS. A. Stratified by age. B. Stratified by hypertension. C. Stratified by cumulative anthracycline dose.

increases the risk of ANTs-induced cardiotoxicity [21]. Patients with hypertension have impaired myocardial reserve function. When receiving ANTs chemotherapy, the risk of left ventricular dysfunction is higher, and the threshold for cardiac insufficiency is lower. For hypertensive patients with left ventricular hypertrophy, this threshold may be as low as 40 mg/m^2 [22]. A considerable proportion of patients in this study cohort had hypertension, which may be an important reason for the high incidence of ARCD, even at cumulative doses of less than 400 mg/m^2. Additionally, the results showed that being aged 65 years or older was associated with an increased risk of ARCD, which is consistent with the conclusions of previous research [23]. These results also suggest that, in addition to the cumulative drug dose, individual patient factors such as age and hypertension can affect the occurrence of ARCD. Therefore, these high-risk groups require more intensive cardiac monitoring. Based on this, the European Society of Cardiology Heart Failure Association (HFA) and the International Cardio-Oncology Society (ICOS) recently proposed a cardiovascular risk stratification system [24]. This system can be used to evaluate patients prior to ANT treatment and incorporates clinical and laboratory risk factors, such as age and hypertension, into a unified scoring model. This allows high-risk groups to be identified and enables the development of personalised cardiac monitoring strategies.

Although the incidence of early cardiotoxicity from ANTs is low, subclinical cardiac injury is not uncommon. Subclinical cardiac injury represents an early stage of cardiotoxicity. Patients do not exhibit an obvious clinical symptoms, but there are early changes in the deterioration of cardiac structure and function [25]. Conventional echocardiographic measurement of LVEF can reflect myocardial contractility; however, it lacks sensitivity in detecting early myocardial damage. This is primarily because compensatory hypercontractility of the adjacent myocardial segments masks the regional wall motion abnormalities, ultimately leading to underestimation of subclinical myocardial injury [26]. Consequently, LVEF is not sensitive enough in the early stage of subclinical heart disease, which can delay diagnosis until irreversible car-

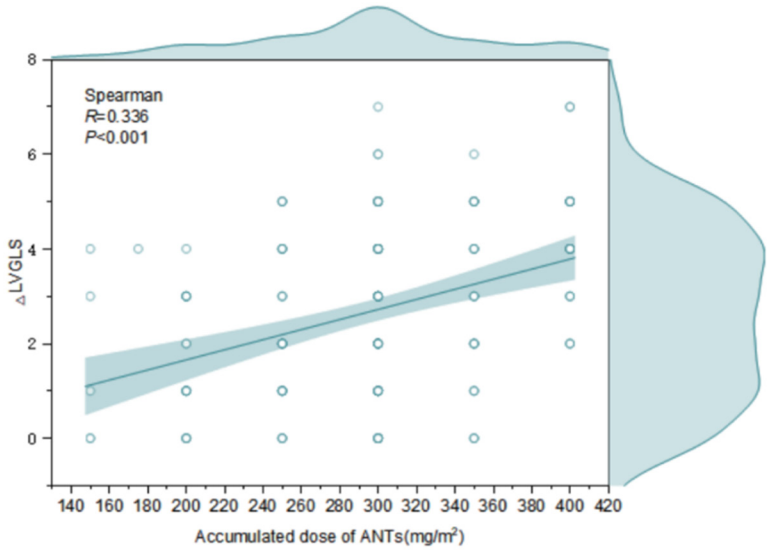

Figure 7. The correlation between ΔLVGLS and cumulative anthracycline dose. Abbreviation: Δ, absolute value of change between T0 and T2; LVGLS, left ventricular global longitudinal strain; ANTs, anthracyclines.

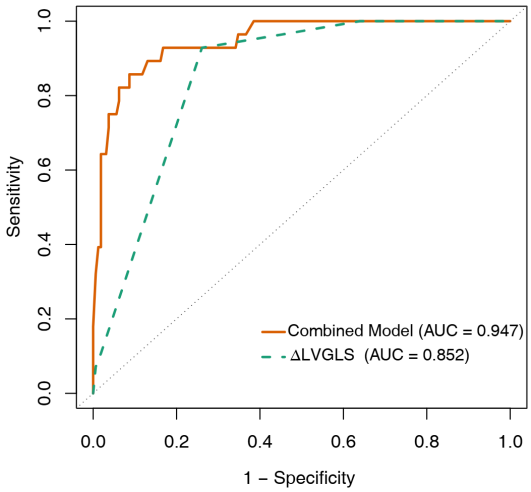

Figure 8. The predictive value of ΔLVGLS and combined with other indicators for ARCD.

diac damage has occurred [27]. Speckle tracking technology provides a quantitative analysis of myocardial strain by tracking the movement of myocardial speckles. It has been shown to be highly effective in detecting subclinical cardiac dysfunction [28]. This study compared the cardiac function and global myocardial strain parameters at T0, T2, and T4 during lymphoma chemotherapy. Compared with commonly used echocardiographic indicators, LVGLS showed early detection at T2, with a significant decrease (P<0.05). GEE analysis further demonstrated distinct longitudinal trajectories between groups, with significant time-by-group interactions at T2 and T4. The ARCD group exhibited a sharp early decline in LVGLS, whereas the non-ARCD group showed minimal change, supporting the early identification value of 3D-STI. This suggests that ANTs may damage the heart in the early stages of chemotherapy.

Further stratified analysis showed that LVGLS at T2 was significantly lower than that at T0 in patients of different ages and genders, suggesting that early ANT-induced cardiotoxicity is a common phenomenon and is not significantly influenced by age or sex. The decrease of LVGLS can be used as a sensitive indicator for early identification of high-risk groups. Consistent with recent evidence in NHL patients treated with R-CHOP, Gimatdinova et al. identified LVGLS reduction as one of the most sensitive indicators of cardiotoxicity [29]. 3D-STI is an advanced echocardiographic technique that evaluates myocardial strain by tracking the three-dimensional movement of the myocardium throughout the cardiac cycle, thereby detecting myocardial injury earlier and more sensitively. Mihalcea et al. [30] studied 110 NHL patients with baseline LVEF >50% who received CHOP chemotherapy and found that three-dimensional LVGLS had decreased significantly from the third course of treatment, while while LVEF showed no significant change. This study further confirmed that, in patients with a cumulative dose of ≥240 mg/m^2, LVGLS at T2 was significantly lower than at T0 and that the change in LVGLS was greater than in patients with a cumulative dose of <240 mg/m^2 (P< 0.05). This indicates that subclinical myocardial injury shows a cumulative effect with increasing ANT exposure, and that LVGLS is a reliable indicator of dose-dependent cardiotoxicity. The predictive value of LVGLS for cardiotoxicity has been consistently demonstrated across diverse populations. In pediatric cancer patients, a relative reduction in LVGLS ≥15% served as the optimal predictor of post-treatment cardiac toxicity [31]. Similarly, in adults with preserved baseline LVEF, a baseline LV-

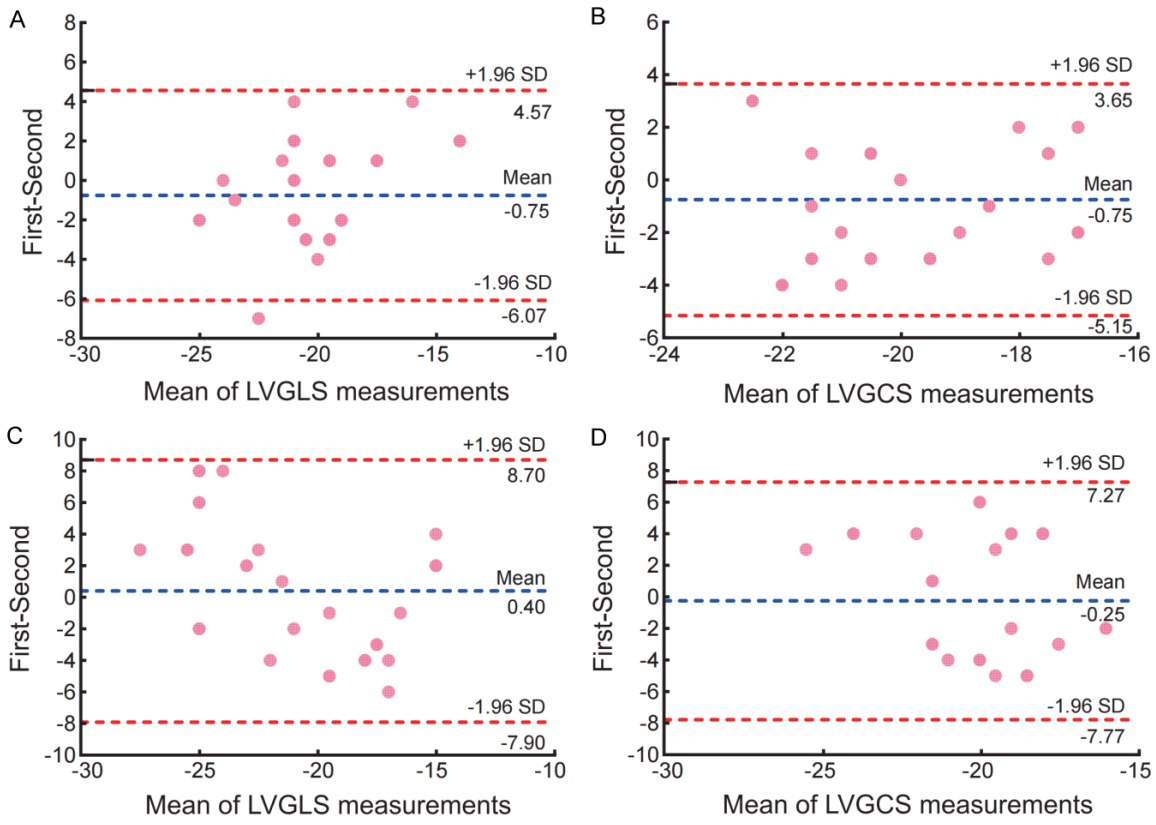

Figure 9. Bland-Altman analysis of reproducibility. A, B. Intra-operator agreement; C, D. Inter-operator agreement. Abbreviation: SD, standard deviation; LVGLS, left ventricular global longitudinal strain; LVGCS, left ventricular global circumferential strain.

GLS ≥ -18% independently predicted subsequent cancer therapy-related cardiac dysfunction [32]. Specifically within the lymphoma population, a baseline LVGLS ≥ -18% has also been identified as the optimal cutoff for predicting post-chemotherapy LV dysfunction [33].

A new study published in 2025 by the American Heart Association pointed out that LVGLS, based on speckle tracking technology, is the most widely used strain parameter in clinical practice and is recommended as an indicator of cardiac function monitoring during cancer chemotherapy [34]. This is consistent with the early LVGLS decline observed in this study. In the three-layer structure of the left ventricular wall, the subendocardial layer, which is responsible for longitudinal contraction and has a relatively lower blood supply, is particularly vulnerable to ischemic injury [35]. Myocardial fibre damage caused by ANTs was also mainly concentrated in this area. This may explain the significant positive correlation observed between ΔLVGLS and the cumulative ANT dose. As the drug dose increased, longitudinal strain injury to the subendocardial layer gradually worsens. In the early stages of the disease, radial and circumferential systolic function may maintain overall cardiac pumping efficiency through compensatory mechanisms. This could be why the LVEF can remain within the normal range in the early stages of the cardiotoxicity. In addition, this study found that the cut-off value of ΔLVGLS in predicting ARCD was 3.5%, with an AUC of 0.852 and respective sensitivity and specificity of 0.929 and 0.739. The AUC was increased to 0.947 by constructing a predictive model that combined ΔLVGLS with age, hypertension, and the cumulative dose of ANTs. The sensitivity and specificity were 0.857 and 0.913. The accuracy of ARCD prediction was significantly improved by the combination of multiple factors, providing quantifiable indicators for early clinical identification of high-risk patients.

Although ANT-induced left ventricular dysfunction has been extensively investigated, its im-

pact on right ventricular function remains relatively less well-studied [36]. In the present cohort, increases in RVEDV and RVESV were observed at the T4 follow-up, suggesting subclinical right ventricular remodeling. However, these parameters did not differentiate between the T0 and T2, limited sensitivity for early detection of right ventricular myocardial injury. This delayed manifestation may be attributed to the unique anatomical characteristics of the right ventricle: its thinner myocardial wall and higher compliance confer greater tolerance to pressure and volume loads compared to the left ventricle [37]. Future studies incorporating additional parameters are warranted to better characterize early changes in right ventricular function.

Limitations

This study has several limitations. First, the inclusion criterion of baseline LVEF ≥55% was applied to evaluate 3D-STI for detecting early subclinical myocardial injury in patients with preserved cardiac function; however, this excludes patients with preexisting cardiac dysfunction, limiting the generalizability of our findings. Second, the limited number of ARCD events constrains the statistical power of multivariable analysis, and some potential risk factors, such as diabetes mellitus and IPI score, could not be fully assessed, leaving the possibility of residual confounding. Third, conventional myocardial injury biomarkers (e.g., troponin, BNP) were not measured, preventing direct comparison between 3D-STI and biochemical indicators. Finally, the 12-month follow-up, while sufficient for capturing early-onset dysfunction, does not allow assessment of the long-term prognostic value of 3D-STI changes for clinical endpoints such as heart failure hospitalization.

Conclusions

ANT-related cardiac dysfunction is significantly associated with advanced age, hypertension, and higher cumulative ANT dose. 3D-STI, and specifically LVGLS, offers significant advantages in the early identification of cardiac dysfunction in lymphoma patients undergoing ANTs treatment.

Disclosure of conflict of interest

None.

Address correspondence to: Qianqian Li and Xiaomei Chen, Department of Cardiac Ultrasound, Qingdao Municipal Hospital, NO. 1, Jiaozhou Road, Qingdao 266000, Shandong, China. Tel: +86-0532-88905330; E-mail: liqianqianqdslyy@126.com (QQL); axiaomeichen@163.com (XMC)

References

[1] Siegel RL, Giaquinto AN and Jemal A. Cancer statistics, 2024. CA Cancer J Clin 2024; 74: 12-49.

[2] Armitage JO, Gascoyne RD, Lunning MA and Cavalli F. Non-Hodgkin lymphoma. Lancet 2017; 390: 298-310.

[3] Anderson E, Choi Y, Buchsbaum RJ, Klein A, Ky B, Landsburg D, Durani U, Ruddy KJ, Yu AF, Leong D, Asnani A, Neilan TG, Ganatra S, Bloom M, Barac A, Yang EH, Deswal A, Cheng RK, Weiss M, Evens AM, Kahl B, Friedberg JW, Parsons SK and Upshaw JN. Hematology-oncology provider perspectives regarding lymphoma treatment and cardioprotective strategies in patients with lymphoma at high risk for heart failure. Leuk Lymphoma 2025; 66: 1437-1446.

[4] Xie S, Sun Y, Zhao X, Xiao Y, Zhou F, Lin L, Wang W, Lin B, Wang Z, Fang Z, Wang L and Zhang Y. An update of the molecular mechanisms underlying anthracycline induced cardiotoxicity. Front Pharmacol 2024; 15: 1406247.

[5] Spadafora L, Di Muro FM, Intonti C, Massa L, Monelli M, Pedretti RFE, Palazzo Adriano E, Guarini P, Cantiello G, Bernardi M, Russo F, Cacciatore S, Sabouret P, Golino M, Biondi Zoccai G, Zimatore FR and Dalla Vecchia LA. Lifestyle and pharmacological interventions to prevent anthracycline-related cardiotoxicity in cancer patients. J Cardiovasc Dev Dis 2025; 12: 212.

[6] Piepoli MF, Hoes AW, Agewall S, Albus C, Brotons C, Catapano AL, Cooney MT, Corrà U, Cosyns B, Deaton C, Graham I, Hall MS, Hobbs FDR, Løchen ML, Löllgen H, Marques-Vidal P, Perk J, Prescott E, Redon J, Richter DJ, Sattar N, Smulders Y, Tiberi M, van der Worp HB, van Dis I, Verschuren WMM and Binno S; ESC Scientific Document Group. 2016 European Guidelines on cardiovascular disease prevention in clinical practice: The Sixth Joint Task Force of the European Society of Cardiology and Other Societies on Cardiovascular Disease Prevention in Clinical Practice (constituted by representatives of 10 societies and by invited experts) Developed with the special contribution of the European Association for Cardiovascular Prevention & Rehabilitation (EACPR). Eur Heart J 2016; 37: 2315-2381.

[7] Iervolino A, Spadafora L, Spadaccio C, Iervolino V, Biondi Zoccai G and Andreotti F. Myocar-

dial cell preservation from potential cardiotoxic drugs: the role of nanotechnologies. Pharmaceutics 2022; 15: 87.
[8] Curigliano G, Cardinale D, Suter T, Plataniotis G, de Azambuja E, Sandri MT, Criscitiello C, Goldhirsch A, Cipolla C and Roila F; ESMO Guidelines Working Group. Cardiovascular toxicity induced by chemotherapy, targeted agents and radiotherapy: ESMO Clinical Practice Guidelines. Ann Oncol 2012; 23 Suppl 7: vii155-66.
[9] Wang C, Zhang R, He J, Yu L, Li X, Zhang J, Li S, Zhang C, Kagan JC, Karp JM and Kuai R. Ultrasound-responsive low-dose doxorubicin liposomes trigger mitochondrial DNA release and activate cGAS-STING-mediated antitumour immunity. Nat Commun 2023; 14: 3877.
[10] Ito-Hagiwara K, Hagiwara J, Endo Y, Becker LB and Hayashida K. Cardioprotective strategies against doxorubicin-induced cardiotoxicity: a review from standard therapies to emerging mitochondrial transplantation. Biomed Pharmacother 2025; 189: 118315.
[11] Migliari M, Fazzini L, Campana N, Deidda M, Dessì M and Cadeddu Dessalvi C. Current strategies for prevention of cancer therapy-related cardiotoxicity: pharmacological, non-pharmacological and emerging approaches. Front Cardiovasc Med 2025; 12: 1668308.
[12] Azzam M, Wasef M, Khalaf H and Al-Habbaa A. 3D-based strain analysis and cardiotoxicity detection in cancer patients received chemotherapy. BMC Cancer 2023; 23: 760.
[13] Piveta RB, Rodrigues ACT, Vieira MLC, Fischer CH, Afonso TR, Daminello E, Cruz FM, Galvão TFG, Filho EBL, Katz M and Morhy SS. Early change in area strain detected by 3D speckle tracking is associated with subsequent cardiotoxicity in patients treated with low doses of anthracyclines. Front Cardiovasc Med 2022; 9: 842532.
[14] Ruppert AS, Dixon JG, Salles G, Wall A, Cunningham D, Poeschel V, Haioun C, Tilly H, Ghesquieres H, Ziepert M, Flament J, Flowers C, Shi Q and Schmitz N. International prognostic indices in diffuse large B-cell lymphoma: a comparison of IPI, R-IPI, and NCCN-IPI. Blood 2020; 135: 2041-2048.
[15] Plana JC, Galderisi M, Barac A, Ewer MS, Ky B, Scherrer-Crosbie M, Ganame J, Sebag IA, Agler DA, Badano LP, Banchs J, Cardinale D, Carver J, Cerqueira M, DeCara JM, Edvardsen T, Flamm SD, Force T, Griffin BP, Jerusalem G, Liu JE, Magalhães A, Marwick T, Sanchez LY, Sicari R, Villarraga HR and Lancellotti P. Expert consensus for multimodality imaging evaluation of adult patients during and after cancer therapy: a report from the American Society of Echocardiography and the European Association of Cardiovascular Imaging. J Am Soc Echocardiogr 2014; 27: 911-39.
[16] Nathan P, Kulkarni K and MacDonald T. Incidence and risk factors of anthracycline-induced cardiotoxicity in long-term survivors of pediatric cancer: a population based cohort study. J Pediatr Hematol Oncol 2022; 7: 136-141.
[17] Camilli M, Ferdinandy P, Salvatorelli E, Menna P and Minotti G. Anthracyclines, diastolic dysfunction and the road to heart failure in cancer survivors: an untold story. Prog Cardiovasc Dis 2024; 86: 38-47.
[18] Bates JE, Howell RM, Liu Q, Yasui Y, Mulrooney DA, Dhakal S, Smith SA, Leisenring WM, Indelicato DJ, Gibson TM, Armstrong GT, Oeffinger KC and Constine LS. Therapy-related cardiac risk in childhood cancer survivors: an analysis of the childhood cancer survivor study. J Clin Oncol 2019; 37: 1090-1101.
[19] Camilli M, Cipolla CM, Dent S, Minotti G and Cardinale DM. Anthracycline cardiotoxicity in adult cancer patients: JACC: CardioOncology State-of-the-Art Review. JACC CardioOncol 2024; 6: 655-677.
[20] Lyon AR, López-Fernández T, Couch LS, Asteggiano R, Aznar MC, Bergler-Klein J, Boriani G, Cardinale D, Cordoba R, Cosyns B, Cutter DJ, de Azambuja E, de Boer RA, Dent SF, Farmakis D, Gevaert SA, Gorog DA, Herrmann J, Lenihan D, Moslehi J, Moura B, Salinger SS, Stephens R, Suter TM, Szmit S, Tamargo J, Thavendiranathan P, Tocchetti CG, van der Meer P and van der Pal HJH; ESC Scientific Document Group. 2022 ESC Guidelines on cardio-oncology developed in collaboration with the European Hematology Association (EHA), the European Society for Therapeutic Radiology and Oncology (ESTRO) and the International Cardio-Oncology Society (IC-OS). Eur Heart J 2022; 43: 4229-4361.
[21] Fabiani I, Chianca M, Cipolla CM and Cardinale DM. Anthracycline-induced cardiomyopathy: risk prediction, prevention and treatment. Nat Rev Cardiol 2025; 22: 551-563.
[22] Tanaka Y, Tanaka H, Hatazawa K, Yamashita K, Sumimoto K, Shono A, Suzuki M, Yokota S, Suto M, Mukai J, Takada H, Matsumoto K, Minami H and Hirata KI. Effect of hypertension on the optimal anthracycline cumulative dose for developing left ventricular dysfunction in patients with malignant lymphoma. Int J Cardiovasc Imaging 2022; 38: 931-939.
[23] Boddicker NJ, Larson MC, Castellino A, Herrmann J, Inwards DJ, Thanarajasingam G, Maurer MJ, Allmer C, Witzig TE, Nowakowski GS, Habermann TM, Villarraga HR, Slager SL, Cerhan JR and Thompson CA. Anthracycline treatment, cardiovascular risk factors and the

cumulative incidence of cardiovascular disease in a cohort of newly diagnosed lymphoma patients from the modern treatment era. Am J Hematol 2021; 96: 979-988.

[24] Lyon AR, Dent S, Stanway S, Earl H, Brezden-Masley C, Cohen-Solal A, Tocchetti CG, Moslehi JJ, Groarke JD, Bergler-Klein J, Khoo V, Tan LL, Anker MS, von Haehling S, Maack C, Pudil R, Barac A, Thavendiranathan P, Ky B, Neilan TG, Belenkov Y, Rosen SD, Iakobishvili Z, Sverdlov AL, Hajjar LA, Macedo AVS, Manisty C, Ciardiello F, Farmakis D, de Boer RA, Skouri H, Suter TM, Cardinale D, Witteles RM, Fradley MG, Herrmann J, Cornell RF, Wechelaker A, Mauro MJ, Milojkovic D, de Lavallade H, Ruschitzka F, Coats AJS, Seferovic PM, Chioncel O, Thum T, Bauersachs J, Andres MS, Wright DJ, López-Fernández T, Plummer C and Lenihan D. Baseline cardiovascular risk assessment in cancer patients scheduled to receive cardiotoxic cancer therapies: a position statement and new risk assessment tools from the Cardio-Oncology Study Group of the Heart Failure Association of the European Society of Cardiology in collaboration with the International Cardio-Oncology Society. Eur J Heart Fail 2020; 22: 1945-1960.

[25] Zheng Y, Liu H, Zhao L, Guan S, Huo H, Li H, Guo J, Peng X, Hao Y, Jin S, Hou Y, Dai X, Liu T and Zhang X. Serial cardiac MRI for quantification of the dynamics of anthracycline-induced subclinical myocardial injury. J Magn Reson Imaging 2023; 58: 1533-1541.

[26] Knight DS, Schwaiger JP, Krupickova S, Davar J, Muthurangu V and Coghlan JG. Accuracy and test-retest reproducibility of two-dimensional knowledge-based volumetric reconstruction of the right ventricle in pulmonary hypertension. J Am Soc Echocardiogr 2015; 28: 989-98.

[27] Dai B, Xu J and Wang B. A meta-analysis of risk factors for cardiovascular adverse events with anthracycline based chemotherapy in lymphoma patients. BMC Cancer 2025; 25: 162.

[28] Niu H, Ma Z, Yang S, Shen X, Ding H and Yuan F. Two-dimensional speckle tracking imaging and tissue Doppler imaging can predict subclinical left ventricular systolic and diastolic dysfunctions after chemotherapy for breast cancer. Am J Transl Res 2025; 17: 1087-1096.

[29] Gimatdinova GR, Danilova OE and Davydkin IL. Biomarkers for monitoring R-CHOP-associated cardiotoxicity in patients with non-Hodgkin lymphoma. Cardiovasc Hematol Disord Drug Targets 2026.

[30] Mihalcea D, Florescu M, Bruja R, Patrascu N, Vladareanu AM and Vinereanu D. 3D echocardiography, arterial stiffness, and biomarkers in early diagnosis and prediction of CHOP-induced cardiotoxicity in non-Hodgkin's lymphoma. Sci Rep 2020; 10: 18473.

[31] Gunsaulus M, Alsaied T, Tersak JM, Friehling E and Rose-Felker K. Abnormal global longitudinal strain during anthracycline treatment predicts future cardiotoxicity in children. Pediatr Cardiol 2024; 45: 1750-1758.

[32] Araujo-Gutierrez R, Chitturi KR, Xu J, Wang Y, Kinder E, Senapati A, Chebrolu LB, Kassi M and Trachtenberg BH. Baseline global longitudinal strain predictive of anthracycline-induced cardiotoxicity. Cardiooncology 2021; 7: 4.

[33] Hatazawa K, Tanaka H, Nonaka A, Takada H, Soga F, Hatani Y, Matsuzoe H, Shimoura H, Ooka J, Sano H, Mochizuki Y, Matsumoto K and Hirata KI. Baseline global longitudinal strain as a predictor of left ventricular dysfunction and hospitalization for heart failure of patients with malignant lymphoma after anthracycline therapy. Circ J 2018; 82: 2566-2574.

[34] Smiseth OA, Rider O, Cvijic M, Valkovič L, Remme EW and Voigt JU. Myocardial strain imaging: theory, current practice, and the future. JACC Cardiovasc Imaging 2025; 18: 340-381.

[35] Chen W, Jiao Z, Li W and Han R. Two-dimensional speckle tracking echocardiography, a powerful method for the evaluation of anthracyclines induced left ventricular insufficiency. Medicine (Baltimore) 2022; 101: e31084.

[36] Song FY, Shi J, Guo Y, Zhang CJ, Xu YC, Zhang QL, Shu XH and Cheng LL. Assessment of biventricular systolic strain derived from the two-dimensional and three-dimensional speckle tracking echocardiography in lymphoma patients after anthracycline therapy. Int J Cardiovasc Imaging 2017; 33: 857-868.

[37] Naeije R and Badagliacca R. The overloaded right heart and ventricular interdependence. Cardiovasc Res 2017; 113: 1474-1485.